

# A new species of Brontotheriidae from the Middle Eocene of Junggar Basin, Xinjiang, China

Li Shuo<sup>1,2</sup>

(1 Key Laboratory of Vertebrate Evolution and Human Origins of Chinese Academy of Sciences, Institute of Vertebrate Paleontology and Paleoanthropology, Chinese Academy of Sciences Beijing 100044 lishuo1001@126.com)  
 (2 University of Chinese Academy of Sciences Beijing 100049)

**Abstract** A new species of large Irdinmanhan brontothere, *Epimanteoceras mae* sp. nov., is described based on an incomplete skull which was collected from the Üqbulak Formation of Sangequan site, Junggar Basin of Xinjiang Uygur Autonomous Region. The new specimen can be assigned to the genus *Epimanteoceras* by the large superorbital processes, the broad frontal bone, the shallow central fossae on the molars, and the absence of the anterolinguinal cingular cusp on molars and the hypocone on M3. *E. mae* is characterized by the slightly laterally bowed zygomatic arches, the medially arched parasagittal ridges, the posteromedially angled external auditory pseudomeatus, and the prominent occipital pillar processes. *E. mae* and *E. formosus* are closely related. It is uncertain whether *E. mae* or *E. formosus* forms the sister group to Brontotheriina, but both of them are the basal group of the latter in the phylogenetic analysis. They are both closer to the Irdinmanhan brontothere *Protitan grangeri* from Nei Mongol but much primitive than *Aktautitan hippopotamopus* from Kazakhstan. The discovery of *E. mae* in Sangequan indicates that the age of Üqbulak Formation is Middle Eocene, and earlier than that of Kyzylbulak Formation bearing *A. hippopotamopus* in Kazakhstan. Moreover, the discovery of *E. mae* in Xinjiang expanded the distribution of the genus *Epimanteoceras*, which was only found in Nei Mongol previously.

**Key words** Junggar Basin, Sangequan, Middle Eocene, *Epimanteoceras*

**Citation** Li S, in press. A new species of Brontotheriidae from the Middle Eocene of Junggar Basin, Xinjiang, China. *Vertebrata PalAsiatica*

## 1 Introduction

The Brontotheriidae is an extinct family of perissodactyls. As one of the most diverse ungulate clades, Brontotheriidae nearly had a Holarctic distribution during the Middle-Late Eocene (Osborn, 1929; Colbert, 1938; Granger and Gregory, 1943; Wang, 1982; Kumar and Sahni, 1985; Qi and Beard, 1996, 1998; Eberle, 2006; Holroyd and Ciochon, 2000; Mihlbachler et al., 2004a; Mihlbachler, 2008; Kazunori et al., 2011) (Fig. 1). Brontotheres occurred in North America at the beginning of the Bridgerian age (Early Eocene); the most primitive brontothere

国家自然科学基金(项目批准号: 41128002)资助。

收稿日期: 2016-12-19

is *Eotitanops* (Osborn, 1907). Brontotheres had a rapid radiation, nearly a half of brontothere genera from North America occurred within about 2 million years during the early Uintan Land Mammal Age (Burger and Tackett, 2014). Brontotheres also immigrated into Asia in a very short time after the occurrence of *Eotitanops* (Missiaen, 2011). Brontotheres had evolved the very large body size and the conspicuous frontonasal horn at the Late Eocene. But they were all extinct at the end of the Late Eocene. Most fossil records of brontothere in Asia are from Nei Mongol and Mongolia (Osborn, 1923, 1925, 1929; Granger and Gregory, 1943; Wang, 1978, 1982, 2000; Ye, 1983; Mihlbachler, 2007). In other regions, the brontothere are scarce and more fragmentary (Wang and Wang, 1997; Mihlbachler et al., 2004a; Emry and Lucas, 2002, 2003; Yanovskaya, 1957; Holroyd and Ciochon, 2000; Thewissen et al., 1987, 2001; West, 1980; Miao, 1982; Wang, 1978; Hu, 1961; Xu and Chiu, 1962; Huang and Zheng, 2004).

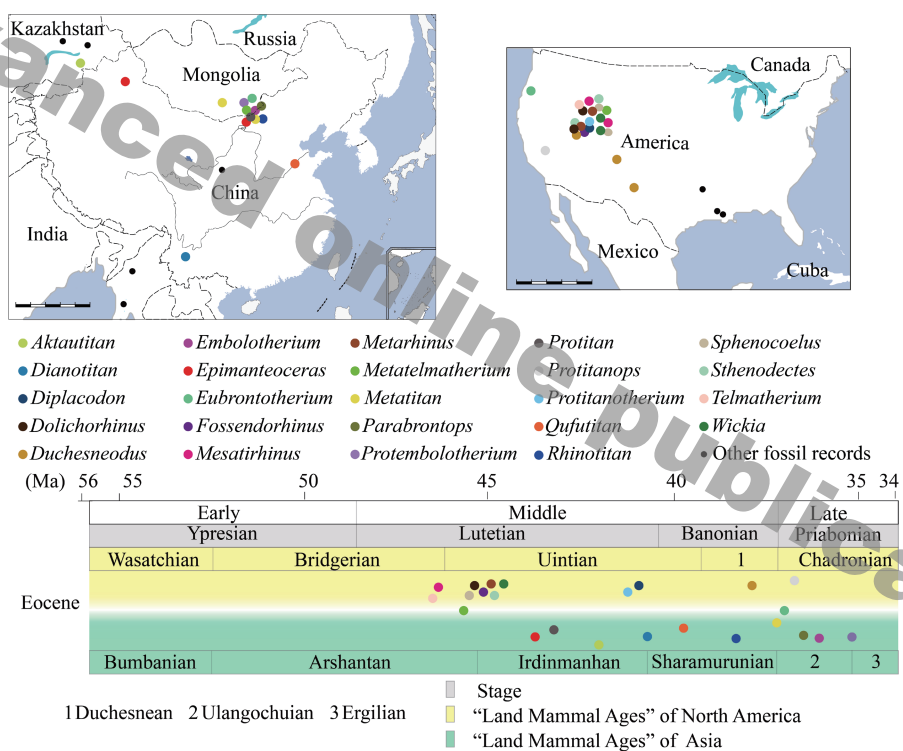


Fig. 1 The geohistorical distribution of Brontotheridae  
scale bar=1000 km

In 2012, the Xinjiang exploration team of IVPP discovered a brontothere skull in Junggar Basin, Xinjiang Uygur Autonomous Region (Fig. 2). This fossil was preserved in the white sandstone-beds of the upper part of the Üqbulak Formation at Sangequan site. Although the facial region (anterior to the orbits) of the skull is missing, it is the best preserved brontothere material from Xinjiang. The new species, *Epimanteoceras mae* sp. nov., described here is the first record of *Epimanteoceras* which was only discovered from Nei Mongol before. The discovery of *E. mae* has increased the species diversity of *Epimanteoceras*, and also has expanded the geographical distribution of the genus.

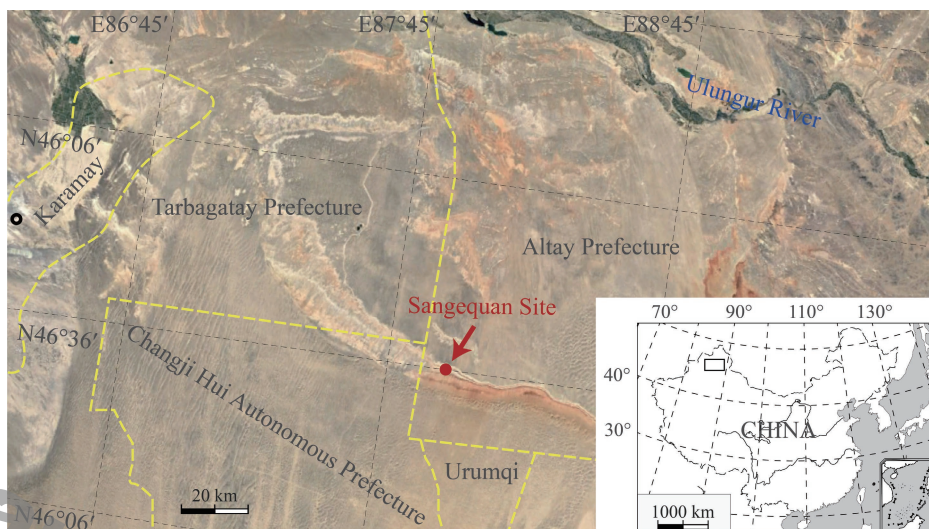


Fig. 2 Map of Xinjiang Uygur Autonomous Region showing the location of Sangequan area  
The spot is showing the collection site of *Epimanteoceras mae* sp. nov.

## 2 Geological Context

The Sangequan site is located in the center of the Junggar Basin, 100 km or so south to the Ulungur River. The Late Cretaceous section and the Eocene section are exposed at the southern cliff here (Tong et al., 1990; Li et al., 2009). The cliff is almost in an east-west extending (Fig. 2). The thickness of the section is about 170 m (Fig. 3). According to the lithologic characters, the section can be divided into the upper part (Üqbulak Formation, about 86 m thick) and the lower part (“Ulungsuhhe” Formation?). The Üqbulak Formation disconformably overlies the “Ulungsuhhe” Formation. The top of the section is covered by the Quaternary conglomerate. The age of Üqbulak Formation is Eocene (Tong et al., 1990). The Üqbulak Formation is consisted beds of grayish white sandstone, dark yellow siltstone and reddish brown mudstone, and yields many large land mammals. The Üqbulak Formation can be divided into 6 horizons. The “Ulungsuhhe” Formation is consisted beds of brownish red mudstone and sandstone. It can be divided into 11 horizons. Bones and eggshells

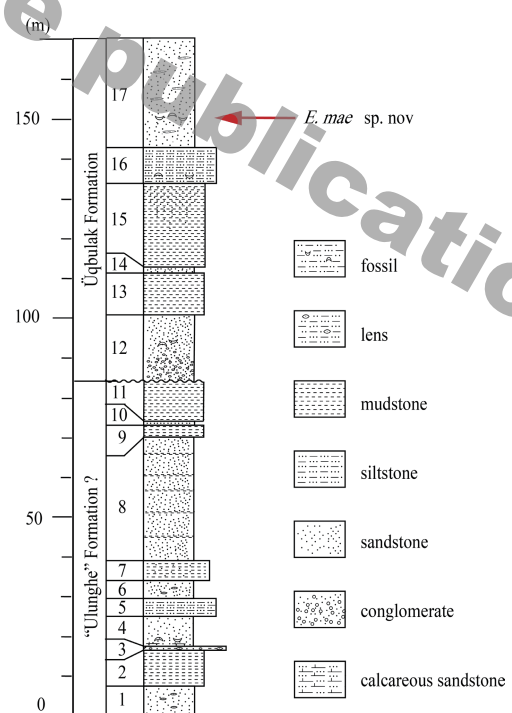


Fig. 3 The stratigraphic column of Sangequan  
The arrow marked the brontothere bone bed

of dinosaurs are yielded from “Ulunguhe” Formation.

The stratigraphic section of Sangequan site (measured by Ye and Bi, personal data).

Quaternary conglomerate

----- Disconformity -----

Üqbulak Formation (86m)

17. Grayish white sandstone with yellow siltstone, containing mammal fossils brontothere, tapiroid and mesonychids	27.5 m
16. Grayish green/yellow siltstone, containing mammal fossils	9 m
15. Brown mudstone, the sand content is increasing upward	21 m
14. Brownish red siltstone	1.5 m
13. Brown mudstone, color greener near the bottom of the bed	10.5 m
12. Yellow sandstone/grayish white sandy conglomerate with grayish white sandstone upwards, containing fragmentary mammal fossils	16.5 m

----- Disconformity -----

“Ulunguhe” Formation ? (84 m)

11. Brownish red mudstone	10 m
10. Well cemented fine sandstone, gray on the concave-convex weathering surface	1 m
9. Brownish red, grayish green on the lower part	3 m
8. Grayish white sandstone, containing grayish green mudstone	31 m
7. Brown mudstone, locally green, brownish red on the weathering surface	5 m
6. Grayish white quartzy fine sandstone, with black massive lenses locally	4.5 m
5. Dark yellow muddy sandstone	4.5 m
4. Light grayish yellow sandstone, grayish white calciferous quartzy fine sandstone on the lower part, containing turtle fossils	7.5 m
3. Light brown argillaceous cemented sandy conglomerate, containing red muddy lenses	1 m
2. Massive brown mudstone	9 m
1. Light yellow medium-fine quartzy sandstone, containing black lenses locally	7.5 m

**Abbreviation:** AMNH, American Museum of Natural History, New York; FMNH, Field Museum of Natural History, Chicago; IVPP, Institute of Vertebrate Paleontology and Paleoanthropology, Chinese Academy of Sciences, Beijing; KAN, Institute of Zoology, Kazak Academy of Sciences, Almaty, Kazakhstan; TMM, Texas Memorial Museum, University of Texas, Austin; YPM, Yale Peabody Museum of Natural History, Yale University, New Haven, Connecticut.

Measurements are taken in millimeters following the method of Mihlbachler (2008) and Froehlich (2002). The terminologies of skull and dentition follow Mihlbachler (2008).

### 3 Systematic paleontology

#### Order Perissodactyla Owen, 1848

#### Family Brontotheriidae Marsh, 1873

#### Subfamily Brontotheriinae Marsh, 1873

#### Tribe Brontotheriina Marsh, 1873

#### Genus *Epimanteoceras* Gregory and Granger, 1943

#### *Epimanteoceras mae* sp. nov.

(Figs. 4–8, Tables 1–2)

**Etymology** Named after the discoverer of the fossil, Ms. Ma Mei.

**Holotype** IVPP V 20713, an incomplete skull (Fig. 4–8) with frontals, parietals, occipital, sphenoids, left M3, detached left M2 and the roots of right M3 but missing the nasals, premaxillae, most part of maxillae and right temporal process of zygomatic bone. Some teeth fragments preserved in the sediment next to the skull are undoubtedly belong to the same individual, including upper incisors (labial part of left I1, lingual part of right I1, labial part of left I2, crown of right I2 and labial part of left I3), premolars (partial crowns) and right M1 (ectoloph). The skull is tilted rightward.

**Type locality** Sangequan site (45°37'39.00"N, 87°58'46.40"E), located in the middle of the Junggar Basin, Xinjiang Uygur Autonomous Region.

**Stratigraphic position and age** Upper part of Üqbulak Formation (Tong, 1989), Middle Eocene (Irdinmanhan).

**Diagnosis** A medium sized brontothere. Compared with *Epimanteoceras formosus*, *E. mae* has the occipital tilting more strongly backward, occipital pillars more distinct with two prominent processes on the upper part, the parasagittal ridges constricting more severely, the external auditory pseudomeatus entering the skull in a more oblique direction (posteromedially) other than a mediolateral direction.

### 4 Description

**Skull** (Figs. 4–7) The holotype of *Epimanteoceras mae* sp. nov. is a posterior half of the skull, missing nasal bone, premaxilla bone and most of maxilla bone. The preserved part of skull is 50 cm in length, measured on the ventral surface from the occipital condyles to the anterior edge of the specimen.

From the dorsal view of V 20713 (Fig. 4), the frontal bones are broad and flat, the dorsal surface of the skull is slightly elevated at the frontal suture (fs). The large triangular superorbital processes are situated above the M3s. The parasagittal ridges (pr) constricted posteriorly but remain separated, the minimum distance between parasagittal ridges is above the paramastoid process. The zygomatic arches are rather thin medial-laterally and lateral bowed slightly. The jugal are straight and divergent posteriorly. The dorsal edges of zygomatic

processes of squamosal (zps) bone are thinner than the ventral edge. The posterior portions of zygomatic processes of temporal bone is anterolaterally protruded, and the angle formed by the posterior portion of zygomatic process of temporal bone and the central line of skull is almost 60°. The dorsal surfaces of the posterior portions of zygomatic process of temporal bone are smooth and anterior sloped. The anterior portions of zygomatic processes of temporal bone are paralleled to the central line of skull with medial angled tips. The frontoparietal suture (fps) is inconspicuous on the dorsal surface of the skull. The surface of the skull on the parietal bone and the occipital bone is fragmentized, the lambdoid suture is unidentified. The sutures between the squamosal portion of the temporal bone and the parietal bone, the squamosal portion of the temporal bone and the occipital bone are clear. The occiput is a bit posterior tilted. The middle portion of the nuchal crest is damaged.

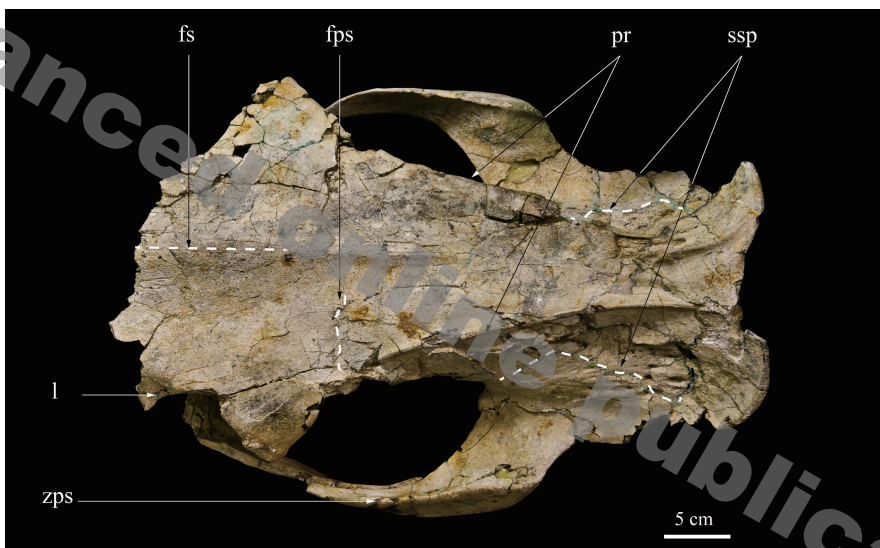


Fig. 4 Dorsal view of *Epimanteoceras mae* sp. nov. (IVPP V 20713)

Abbreviations: fps. frontoparietal suture; fs. frontal suture; l. lacrimal bone; pr. parasagittal ridges;

ssp. sutures between the squamosal portion of the temporal bone and the parietal bone;

zps. zygomatic process of squamosal bone

Table 1 The measurements of the skull of *Epimanteoceras mae* sp. nov. (IVPP V 20713) (mm)

	Skull width	Width between orbits	Width between superorbital processes	Occipital width
<i>Epimanteoceras mae</i>	355	200	310	220

Notes: skull width: maximal skull width measured across the maximum span of the zygomatic arches; width between superorbital processes: measured between the two tips of the superorbital processes; width between orbits: measured between the dorsal edges of the orbits; occipital width: measured between the two ends of the nuchal crest.

From the occipital view of the skull (V 20713, Fig. 5), the nuchal crest is thin and arc-shaped. The dorsal portion (at the nuchal crest) of the occiput is as wide as the ventral portion (at the external auditory pseudomeatus). The width is greater than the height, the ratio of the width and the height is 1.91 (the height is 11.5 cm). The distinct suture between the exoccipital bone

and the supraoccipital bone (so) started from the occipital side of the paramastoid process and dorsally stretched, paralleled to the nuchal crest at the dorsal side of the occipital condyle and slightly concaved downward at the area above the foramen magnum. The occipital condyles are large (the width is 17.5 cm, the height is 7.2 cm), compressed hemisphere-shaped, the surface of the occipital condyles is rough. The occipital pillars (op) are prominent above the occipital condyles. A V-shaped structure is formed by the two occipital pillars on the occiput. A prominent ligule-shaped process is occipitally protruded on the dorsal part of each occipital pillar. The distance of two occipital pillar processes (opp) is as width as the occipital condyles.

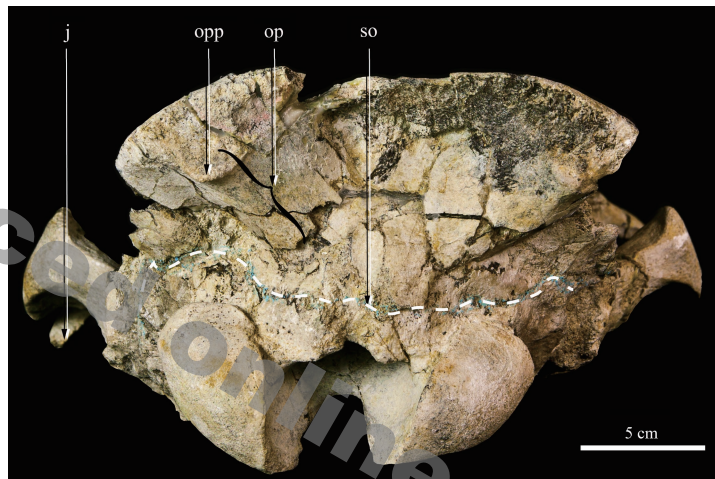


Fig. 5 Occipital view of *Epimanteoceras mae* sp. nov. (IVPP V 20713)

Abbreviations: j. jugal; op. occipital pillar; opp. occipital pillar process; so. suture between the exoccipital bone and the supraoccipital bone

From the lateral view of V 20713 (Fig. 6), the remaining portion of the lacrimal bone (l) is tiny. The surface of the lacrimal bone is rather smooth. The suture of the lacrimal bone and the frontal bone is zigzag-shaped and the posterior portion remains. The orbits (o) are large and ellipse-shaped, positioned above the anterior portion of M3 and the posterior portion of M2. The angle made by the long axis of the orbits and the outline of dorsal surface of the skull is about 30–45°. The superorbital processes (sop) are extending laterally and with slight downward angled tips. The zygomatic arches are rather long, the lengths of the zygomatic arches, from the anterior rim (above the anterior portion of M3 and the posterior portion of M2) to the posterior rim (the anterior rim of the external auditory pseudomeatus), are about 35 cm. The surface of the zygomatic arches is smooth. The squamosal process of the jugal bone (spj) is slender bearing a straight ventral edge. The ventral zygomatic flange seen in *Metatelmatherium* is absent. The frontal processes of jugal bone (fpj), which are disconnected with the superorbital processes, are small triangular processes. They are positioned above the mesostyle of M3, and their contact surface is rather long. The outlines of the ventral side of the squamosal process of the jugal bone and the zygomatic process of the squamosal bone

formed an angle of about 135°, it gave the zygomatic arches a dorsally angled appearance. The postzygomatic process, as seen in *Protitan*, is absent. The transection of the zygomatic process of the temporal bone is triangle-shaped. The ventral surface of the zygomatic process of the temporal bone is rough. The postglenoid processes (pgp) are rather large and oval-shaped or long ellipse-shaped with a narrower medial end than the lateral end. The posttympanic process (ptp) and mastoid process are fused together. The paramastoid processes (pp) are as long as postglenoid processes with somewhat damaged apexes. The postglenoid processes and the posttympanic process are widely separated and formed a ventrally unconstructed external auditory pseudomeatus. There are many ellipse-shaped nutrient foramina distributed along the sutures. The nutrient foramina are successively lengthened anteroposteriorly. The long axes of nutrient foramina are paralleled to the length of the skull.



Fig. 6 Left view of *Epimanteoceras mae* sp. nov. (IVPP V 20713)

Abbreviations: fpj. frontal processes of jugal bone; l. lacrimal bone; nc. nuchal crest; o. orbit; opp. occipital pillar process; pgp. postglenoid process; pp. paramastoid processes; ptp. posttympanic process; s. sphenoid bone; sop. superorbital process; spj. squamosal process of the jugal bone

From the ventral view of V 20713 (Fig. 7), because of the ventral surface of the skull is rather crushed, the suture of sphenoid bone and temporal bone is unidentified. The posterior narial canal (pn) is rather long. The anterior margin of the posterior nares is positioned between the protocones of M3s; the posterior margin of which is positioned between the postglenoid processes. The anterior portion of the posterior nares is rimmed by a moderate wide U-shaped emargination (e). The pterygoid process is long and extending posteriorly to the suture of the sphenoid bone and the occipital bone. The surface of the inner wall of the pterygoid process is smooth. The maxilloturbinate exposed in choanae and extended after the anterior rim of the posterior nares, but they are all combined into a wavy layer of bone in the thin posterior nares pouches. The vomer (v) is rather thin. The posterior part of the vomer has a Y-shaped divarication which is short and with a tiny fossa between the two branches. The ventral sphenoidal fossae (large pits in the ventral surface of the sphenoid seen in *Protitan*,

*Metatitan* and *Diplacodon*), which are continuous with the ventral narial canal are absent. The posterior opening of alisphenoid canal (ac) is positioned at the posterior end of the vomer and opened posteriorly. The foramen ovale (fo) is positioned on the posterior part of the sphenoid bone, behind the pterygoid canal. The aperture of the foramen ovale is opened anteriorly. The foramina lacerum (fl) are positioned at the medial side of the external auditory pseudomeatus (eap), separated far from the foramen ovale. The sphenoid bone and basioccipital bone are connected at the medial side of the foramina lacerum. The external auditory pseudomeatus are anterior to the foramen magnum with a distance of 6 cm separating them. The external auditory pseudomeatus enter the skull in a more oblique posteromedial direction; the angle of the external auditory pseudomeatus and the long axis of skull is about 60°. The small hypoglossal canals (hc) are positioned between the occipital condyles and the foramina lacerum, medial to the processus paramastoideus. The aperture of the hypoglossal canal is opened ventrolaterally.

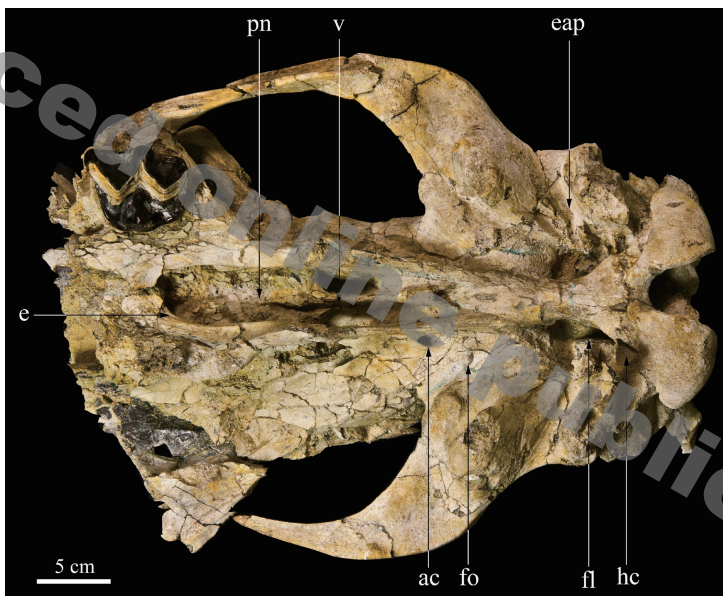


Fig. 7 Ventral view of *Epimanteoceras mae* sp. nov. (IVPP V 20713)

Abbreviations: ac. alisphenoid canal; e. emarginations; eap. external auditory pseudomeatus; fl. foramina lacerum; fo. foramen ovale; hc. hypoglossal canal; pn. posterior nares; v. vomer

**Upper dentition** (Fig. 8) The remaining teeth of the specimen (V 20713) are left M3, incomplete left M2, fragmentary incisors and fragmentary premolars. The left M3 is the only tooth preserved on the maxilla bone. The left M2 is missing mesiolabial portion (the parastyle and the paracone).

The incisors are relative large and successively enlarged from I1 to I3 (Fig. 8 A–E, Table 2).

I1 is subcaniniform or quadrihedron-shaped, but only the labial portion of left I1 (Fig. 8A) and the lingual portion of the right I1 (Fig. 8B) are retained, and rather worn. The lingual cingulum is V-shaped, but no labial cingulum is present. The distal branch of lingual cingulum is short and robust, and the mesial branch is long and slender.

**Table 2** The measurements of *Epimanteoceras mae* sp. nov. and the comparison with several *Indinmanhan* and *Bridgerian* brontotheres (mm)

	II		12		13		C		P1		P2		P3		P4		M1		M2		M3		W/L		M1-M3	
	L	W	L	W	L	W	L	W	L	W	L	W	L	W	L	W	L	W	L	W	M	M2	M3	165 <sup>(3)</sup>	355	
<i>Epimanteoceras mae</i>	14.3	14.5	14.3	14.5	13.3	18.8	16.9	32.7	16.7	10.7	26.2	28.8	26.6	32.8	28.6	36.5	38.6	44.1	54.0	53.0	70.4	52.0	0.98	0.74	158	395
<i>Epimanteoceras formosus</i> <sup>(1)</sup>	13.4	14.3	14.5	14.3	13.3	18.8	16.9	32.7	16.7	10.7	26.3	28.7	26.3	32.8	28.6	36.5	38.6	44.1	54.0	53.0	70.4	52.0	0.98	0.74	158	395
<i>Protitan grangeri</i> <sup>(1)</sup>	12.8	14.8	14.8	15	18.7	17.2	23.1	16.7	11.8	25.3	25.6	27.1	31.0	29.6	35.4	44.7	42.2	66.6	54.4	73.6	60.6	0.82	0.82	171	346	
<i>Protitan minor</i> <sup>(1)</sup>	12.3	12.3	14.8	15.2	19.7	16.4	17	10.4	23.3	23.3	28.0	30.0	28.8	36.2	43.2	45.2	62.3	56.1	67.6	57.1	0.9	0.84	160	300		
<i>Metaelmatherium ultimum</i> <sup>(1)</sup>	14.5	16.3	15.4	16.6	20.4	19.4	25.6	19.3	11.8	22.2	22.1	24.1	27.9	27.1	33.5	42.8	42.7	53.9	53.1	50.9	51	0.99	1	131	293	
<i>Aktauitan hippo</i> <sup>(2)</sup>	16.1	17.9	20.8	23.6	24.6	23.6	26.9	17.7	15.7	28.7	28.7	36.1	35.7	42.9	45.4	57.1	57	83	68.5	97.7	0.83	227				
<i>Telmatherium validus</i> <sup>(1)</sup>	11.2	10.9	13.5	12.4	15.5	13.1	26.8	16.7	10.6	21.3	19.1	21.2	24.3	23.7	29.1	33	33.9	45.8	42.4	47.1	44.5	0.93	0.94	114	295	

Notes: (1) the mean value of the measurements from MihlböHLER (2004); (2) the mean value of the measurements from MihlböHLER (2008); (3) Estimated according the ectoloph of the 3 molars (Fig. 7F-H). L. The maximum mesiodistal length of the molar, measured on the labial side; W. Labiolingual width of the molar, measured from the labial margin of the mesostyle to the lingual margin of the protocone.

I2 is subcaniniform. Only the labial portion of left I2 (Fig. 8C) and the crown of right I2 remain (Fig. 8D), more weakly worn than I1s. Two ridges divided the crown into the labial and the lingual sides. The crown is flat lingually and swollen labially. The labial cingulum is absent.

I3 is subcaniniform, half of the left I3 remains (Fig. 8E). The crown is higher than that of I2.

Because of the missing of the rostrum portion, the shape of incisor row of V 20713 is unknown. The diastema between incisors, I3 and canine, canine and P1, P1 and P2 are also unknown.

Only the ectoloph of the right M1 is preserved (Fig. 8F). The left M2 lacks parastyle, half mesostyle and paracone. The right M3 is broken off, retaining the roots in the maxilla bone. The left M3 is the only complete molar remained in the maxilla bone (Fig. 7).

M2 is quadrangular (Fig. 8G), and moderately worn. The ectoloph is W-shaped, tall and tilted lingually. The ribs on the distal labial surface of the ectoloph are very weak. The metacone included in the ectoloph is wedge-shaped. The mesostyle is developed but the metastyle is weak. The protocone and the hypocone are conical. The protocone is situated near the middle point of the lingual edge and only left a round-shaped wear surface. The hypocone, situated on the distolingual corner of the crown, is much smaller than protocone in size. The wear surface is long ellipse in shape. The protoconule and the metaconule are absent. The central fossa is shallow and triangular. The labial cingulum is weak but slightly developed near the metastyle. The mesial cingulum is thin with a strip-shaped wear surface. The lingual cingulum is developed anterior to the protocone, absent posterior to the protocone. The distal cingulum is very weak or absent.

M3 is similar to M2 in morphology (Fig. 8H) but slightly larger (Table 2). It is less worn than M2. The paracone and metacone are comparable in size. The mesostyle are more developed than in M2. The metastyle is weaker than parastyle and mesostyle. The protocone is a tall conical cusp and situated at the same place as it is in M2. The enamel of the protocone is almost unworn. The hypocone is absent in M3. The shallow, triangular central fossa is present. The mesial cingulum is weaker than in M2. The distal cingulum is relative thick. The labial cingulum is very weak and vanished under the mesostyle. The lingual cingulum is absent. The anterolingular cingular cusp is absent.

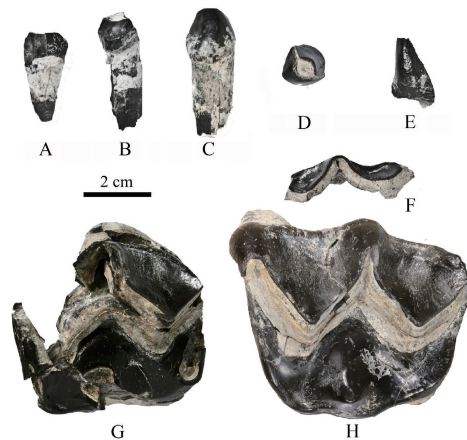


Fig. 8 The upper teeth of *Epimanteoceras mae* sp. nov. (IVPP V 20713)

A. labial portion of left I1; B. lingual portion of right I1; C. labial portion of left I2; D. the crown of right I2; E. labial portion of left I3; F. ectoloph of right M1; G. left M2; H. left M3

## 5 Comparison

The specimen (V 20713) is assigned to *Epimanteoceras* in this paper. *Epimanteoceras formosus* was first described from a single specimen (AMNH 21613) by Granger and Gregory (1943). Another specimen, AMNH 21607, which is remarkably similar to *E. formosus* mentioned by Granger and Gregory (1943), was considered as the new taxa, *Dolichorhinoides angustidens*. The two other species, *E. praecursor* (Yanovskaya, 1953) and *E. amplus* (Yanovskaya, 1976), are considered as the invalid species (Mihlbachler, 2008). *E. formosus* is the only valid species of *Epimanteoceras* so far.

The specimen (V 20713) is assigned to *Epimanteoceras* based on the following characters: 1) the frontal bone is flat and broadened, with large superorbital processes; 2) from lateral views, the occiputs tilt backward and surpass the occipital condyles (Fig. 6); 3) the parasagittal ridges strongly constrict on the dorsal surface of the cranium, but still separate posteriorly and do not merge into a real sagittal crest; 4) the orbits are positioned above the posterior portion of M2 and the anterior portion of M3; 5) from lateral views of the skull, the temporal process of the zygomatic bone is horizontal while the zygomatic process of the temporal bone is sloped posterodorsally, which give the zygomatic arches a curved appearance; 6) the postglenoid process and the mastoid process are unconstricted ventrally and form broad, ventrally opened external auditory pseudomeatus; 7) the incisors are subcaniniform; 8) the anterolinguinal cingular cusps are absent in the molars; 9) the hypocone is absent in M3. In addition, the material is the same size as *E. formosus* (AMNH 21613), the only one species of this genus before now (Table 2).

The specimen is a new species of *Epimanteoceras*. The differences between *E. mae* sp. nov. and *E. formosus* are: 1) the posterior portions of parasagittal ridges in new species are bowed medially, whereas in *E. formosus* the posterior portions of parasagittal ridges are almost parallel; 2) the temporal ridge in the new species is absent or weaker than that in *E. formosus*; 3) from a dorsal view, the zygomatic arches of *E. mae* are arched stronger than that in *E. formosus* laterally; 4) the occipital pillars with tongue-shaped processes of *E. mae* are much robuster than those of *E. formosus*; 5) the occipital condyles of *E. mae* are larger than that in *E. formosus*; 6) the external auditory pseudomeatus of *E. mae* enters the skull in a posteromedial direction, while in *E. formosus*, the external auditory pseudomeatus enters in a medialateral direction.

*Protitan* is an Irdinmanhan brontothere genus from Nei Mongol (Osborn, 1923). It is similar to *E. mae* in the profile and the dentition. *Protitan* includes two valid species (Mihlbachler, 2008), *P. grangeri* (Osborn, 1925) and *P. minor* (Granger and Gregory, 1943). *E. mae* differs from *P. grangeri* (AMNH 20103) and *P. minor* (AMNH 26416) in having a smaller size, broad frontal bone, large superorbital processes, more curved zygomatic arches, the absence of postzygomatic processes and ventral sphenoidal fossae. Additionally, *E. mae* also differs from *P. grangeri* in the more posteromedially angled external auditory pseudomeatus. The curved zygomatic arch is the

plesiomorph character to all the species of *Protitan*.

*Aktautitan hippopotamopus* (Mihlbachler et al., 2004) is an Irdinmanhan brontothere from Ily Basin of Kazakhstan. Its geographical positions is rather closed to that of *E. mae*; but the morphological differences between them are quiet large. *E. mae* differs from *A. hippopotamopus* (KAN N2/875) in having posterior strongly constricted parasagittal ridges, posterior positioned orbits (positioned above M2 in *A. hippopotamopus*), large superorbital processes, curved zygomatic arches, ventrally opened and more posteromedially angled external auditory pseudomeatus (ventrally closed and tubular shaped in *A. hippopotamopus*), caniniform incisors (globular I1 and I2 in *A. hippopotamopus*), presence of hypocone in M3. All but the more posteriorly positioned orbits and the presence of hypocone in M3 are plesiomorph characters.

The Late Bridgerian *Telmatherium validus* (Marsh, 1872) from North America was widely regarded as the ancestor or sister taxon of horned brontotheres of North America and Asia (Granger and Gregory, 1943; Mader, 1989, 1998). It is similar to *E. mae* in profile but smaller in size (Tables 1, 2). The new species is more advanced than *T. validus* (YPM 11120, AMNH 12678 and AMNH 1570) in having posteriorly weakly constricted parasagittal ridges (compared to the primitive genus as *Eotitanops* and *Palaeosyops*), posteriorly positioned anterior margin of the posterior nares (anterior to the protocones of M3s and near to the posterior margin of M2 in *T. validus*) and presence of central molar fossae. Additionally, *E. mae* also differs from *T. validus* in broadened frontal bone, large superorbital processes, posteriorly positioned orbits (also positioned above M2 in *T. validus*) and more posteromedially angled external auditory pseudomeatus.

*Metatelmatherium ultimum* (Granger and Gregory, 1938) is a genus discovered from both North American and Asia (Granger and Gregory, 1943). The Asiatic specimen was discovered in the vicinity of Camp Margetts, the stratum from which the specimen was collected is of Arshantan (Wang et al., 2010). Despite of the primitiveness in evolution, *M. ultimum* is the only certain species whose living age is earlier than *Epimanteoceras* in Asia so far. *E. mae* is more advanced than *M. ultimum* (AMNH 2060) in widened occiput, posteriorly weakly constricted parasagittal ridges (compared to the primitive genus as *Eotitanops* and *Palaeosyops*) and presence of central fossae on molars. It also differs from *M. ultimum* in having a bigger body size, broadened frontal bone, large superorbital processes, more posteromedially angled external auditory pseudomeatus, lacking the zygomatic ventral flange and absence of the molar anterolingual cingular cusps.

The North American *Protitanotherium emarginatum* (Hatcher, 1895) from late Uintan is similar to *E. mae* in profile except the nasal portion. *E. mae* is more primitive than *Pr. emarginatum* (TMM 41723) in curved zygomatic arches, ventral opened external auditory pseudomeatus (ventrally closed and tubular shaped in *Pr. emarginatum*) and caniniform incisors (all are globular in *Pr. emarginatum*). It also differs from *Pr. emarginatum* in having large superorbital processes, posteriorly positioned orbits (also positioned above M2 in *Pr. emarginatum*).

Another North American late Uintan *Diplacodon elatus* (FMNH P14632, P14633) (Marsh, 1875) is also similar to *E. mae* in profile except the nasal portion. *E. mae* is more primitive than *D. elatus* in curved zygomatic arches, ventrally opened external auditory pseudomeatus (ventral closed and tubular shaped in *D. elatus*) and all caniniform incisors (only I3 is caniniform in *D. elatus*). It also differs from *D. elatus* in having somewhat strongly constricted parasagittal ridges, posteriorly positioned orbits (also positioned above M2 in *D. elatus*), the absence of ventral sphenoidal fossae.

## 6 Phylogenetic analysis

To assess the phylogenetic position of *Epimanteoceras mae*, a phylogenetic analysis is performed using the data matrix of Mihlbachler (2008) with addition of the new species (Appendix I). The matrix included 52 taxa and 87 characters. Taxa of *Hyracotherium*, *Pachynolophus*, *Danjiangia* and *Lambdotherium* are also referred as outgroup in this paper. The phylogenetic analysis is performed using traditional search under TNT (version 1.1), equal weighted of all characters. All of the characters are ordered except for character 26 and character 73. The analysis generated 72 parsimonious trees with a tree length of 311 steps, a consistency index of 0.450, and a retention index of 0.813.

The strict consensus tree of 72 most parsimonious trees (Fig. 9) is nearly identical to that of Mihlbachler (2008). *E. mae* is deeply nested within Brontotheriini and shares with other members of Brontotheriini the following optimized apomorphies (Mihlbachler, 2008): a pair of triangular processes of frontal bone that overlapping onto or intruding into the nasal bone, and reduced occipital condyles. In the strict consensus tree (Fig. 9), *E. mae* nested within the polytomic construction (*Nanotitanops shanghuangensis* (Qi and Beard, 1996)-*E. formosus*) that also exhibited by Mihlbachler (2008).

Because of the collapse of the polytomic construction (*Nanotitanops shanghuangensis*-*Epimanteoceras mae*), the phylogenetic position of *E. mae* in Brontotheriini cannot be assessed. To find out the problematic taxa within the polytomy, the script “IterPCR” is run under TNT. The result is identical to that of Mihlbachler (2008), the problematic taxon within the polytomic construction, *N. shanghuangensis*-*E. mae*, is also *N. shanghuangensis* (Fig. 10) (the other problematic taxon, *N. mississippensis* within Brontotheriita (node 5 in Fig. 10), is irrelevant to our new species). The Jiangsu brontothere, *N. shanghuangensis*, lacks the skull data and only being known from a few isolated teeth. The teeth of *N. shanghuangensis* are smaller than *Eotitanops* and *Palaeosyops* in size but much more advanced in dental morphology (Mihlbachler, 2008); the dental morphology of *N. shanghuangensis* is similar to *Epimanteoceras* or even to the genus *Rhinotitan*. As the possible sister taxon to *E. formosus* or the Brontotheriina, *N. shanghuangensis* takes an uncertain position within or outside of the Brontotheriina; the result of this situation generates a polytomic construction at the position near the node Brontotheriina (node 4 in Fig. 10).



Fig. 9 Strict component consensus of traditional search performed with ordered multistate characters

The resulting summary tree (Fig. 10) is the derivative of the strict reduced consensus trees with the problematic taxa (*N. shanghuangensis* and *N. mississippensis*) removed. The resulting summary tree is also identical to that of Mihlbachler (2008). The positions of the taxa within the polytomic construction are ascertained in this tree. In the summary tree, *E. mae* forms a trifurcated branch with *E. formosus* and the monophyletic clade Brontotheriina (node 4 in Fig. 10). *E. mae* and *E. formosus* are primitive to Brontotheriina in lack of the conspicuous frontonasal protuberances (Mihlbachler, 2008).

Although *E. mae* does not form a monophyletic clade with *E. formosus*, the proofs both derived from the morphology (the combination of the features, such as the larger superorbital

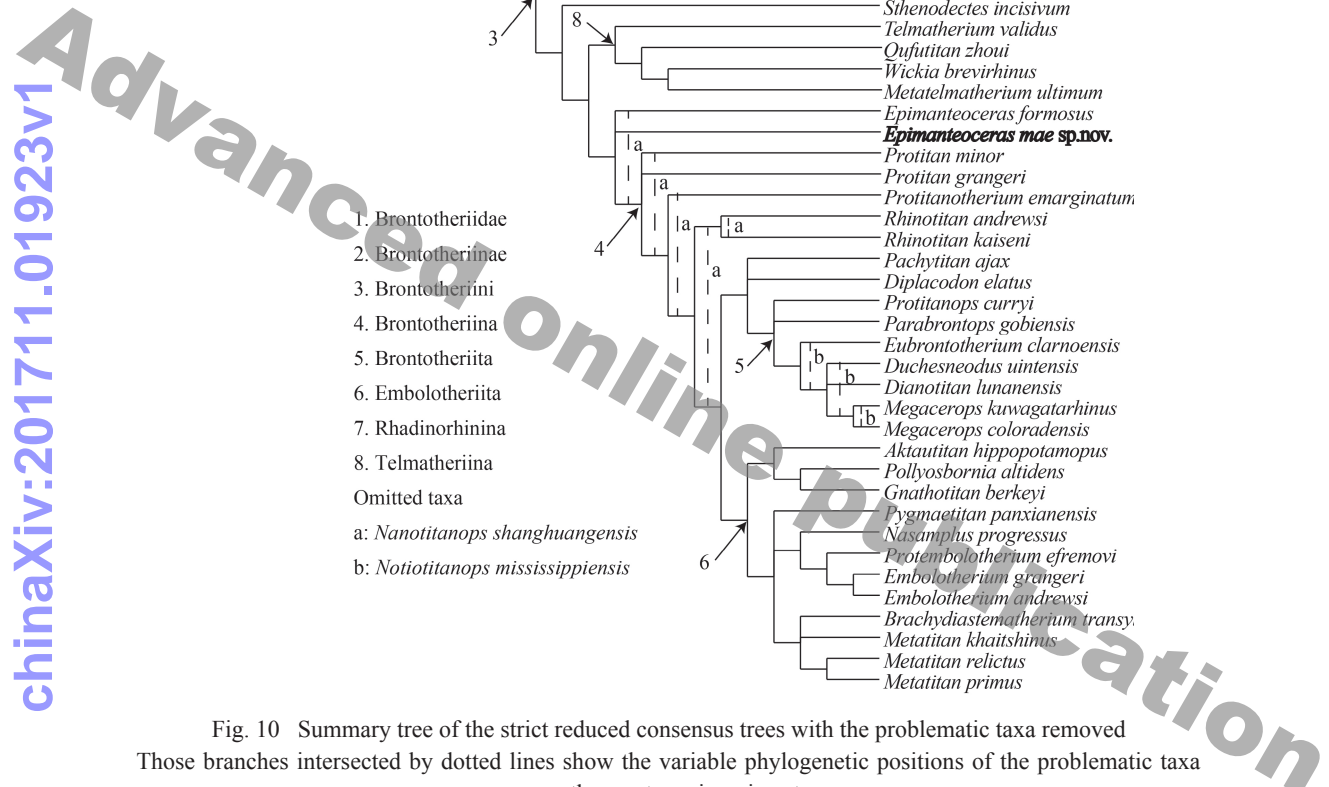


Fig. 10 Summary tree of the strict reduced consensus trees with the problematic taxa removed. Those branches intersected by dotted lines show the variable phylogenetic positions of the problematic taxa among the most parsimonious trees

process, broadened frontal bone, strongly constricted parasagittal ridges, posterior dorsally curved zygomatic arches, absence of anterolingual cingular cusps on the molar and absence of hypocone in M3) and the phylogeny are sufficient to prove that *E. mae* should be assigned into the genus *Epimanteocera*. The reasons why the two species of *Epimanteocera* do not form a monophyletic clade are probably attributed to the lack of following important synapomorphy features caused by the missing of facial portion of the skull: 1) the inconspicuous frontonasal protuberances (character 3: state 2); 2) a more complex P1 that includes distinct paracone and metacone (character 47: state 1); 3) the premolar hypocones and the protocones situated closely and connected by lingual crests (character 53: state 2). Furthermore, the feature of the genus *Epimanteocera*, larger superorbital process (Granger and Gregory, 1943), was not

included in the matrix data by Mihlbachler (2008). The large superorbital processes are only seen in *E. formosus*; and superorbital processes are rather small or inconspicuous in other brontothere taxa. Unfortunately, only two specimens of *E. formosus* have been found so far, and moreover, the superorbital processes are missing in one of the specimen (AMNH 21607). So the genus feature of *Epimanteocera*, larger superorbital process, cannot be added into the matrix. But it would be a good character if more specimens of *Epimanteocera* were present. Besides of the differences between *E. mae* and *E. formosus*, the long distance between the two sites where they were collected is another reason for the creation of the new species.

## 7 Discussion about the age of strata

The fossils of Sangequan area were mainly found in Huashigou (fossil gully) site previously, west to the brontothere bone bed (Tong, 1989a, b; Tong et al., 1990; Wei and Tong, 1992; Li et al., 2009). Tong (1989a) also used “Üqbulak Formation” as the name of the upper strata. The color of Üqbulak Formation is relatively lighter than the lower strata. Three fossil sites were found in Huashigou site in the past (Tong, 1989a): 82507A, 82507B and 82507C (from bottom to top). The Irdinmanhan tapir *Rhodopagus* was found at 82507C (Tong, 1989a). The fauna of the lower fossil site 82507B contains *Breviodon minutus*, *Schlosseria magister*, *Uintatherium cf. insperatus*, *Metacoryphodon* sp., *Pantolamddodon* sp. and cf. *Mesonyx uqbulakensis* (Tong, 1989a). All of these animals are large Middle Eocene land mammals. The fossils from lowest site 82507A are rather fragmental, only *Hyopsodus* can be confirmed (Tong, 1989a).

The brontothere fossiliferous layer is located about 13 km west to the Huashigou. It can easily be traced from this fossiliferous layer to the Huashigou site. *Epimanteoceras mae* was excavated from the top layer of the Üqbulak Formation which is comparable to the layer where the site 82507C locates. The Sangequan brontothere is somewhat plesiomorph to the Irdinmanhan brontothere *Protitan* from Nei Mongol in evolution as *E. formosus*. Together with the animal from the site 82507C (Tong, 1989a), *Rhodopagus*, the discovery of *E. mae* in Sangequan indicates an Irdinmanhan age of the Üqbulak Formation, Middle Eocene, which supports the previous conclusion (Tong, 1989a). Additionally, the Kazakhstan Irdinmanhan brontothere, *Aktautitan hippopotamopus*, is more advanced than *E. mae* in evolutionary level therefore the age of the strata from which the Kazakhstan’s *Aktautitan hippopotamopus* yielded is younger than Üqbulak Formation of Sangequan.

**Acknowledgements** I am grateful to my supervisor Dr. Bi Shundong for guiding in my research, to Ms. Ma Mei for providing the specimen. I thank Prof. Wu Wenyu and Ye Jie for their constructive suggestions and comments. I thank Prof. Wu Wenyu for English improvement; Gao Wei for photography; Li Shijie for the help of fossil repair, and the teachers of the Collection House of IVPP for supporting the material for my comparison.

## 准噶尔盆地三个泉始新世雷兽（奇蹄目、雷兽科）一新种

李 硕<sup>1,2</sup>

(1 中国科学院古脊椎动物与古人类研究所, 中国科学院脊椎动物演化与人类起源重点实验室 北京100044)

(2 中国科学院大学 北京100049)

**摘要:** 新疆准噶尔盆地三个泉中始新世依希白拉组内发现的晚叉额雷兽属新种—马氏晚叉额雷兽(*Epimanteoceras mae* sp. nov.)是新疆目前发现保存最好的雷兽头骨化石。标本为一件不完整的头骨, 缺失鼻骨, 前颌骨, 部分上颌骨和泪骨。新种具有眶上突较粗大, 额骨宽阔平坦, 白齿有中心窝, 白齿舌侧齿带前部上的齿尖不发育, M3无次尖等晚叉额雷兽属的特征。新种的颧弓成向外扩的弓形, 额顶嵴在后侧向内收缩弯曲的弧度更大, 外耳道较为倾斜, 枕柱上方有舌状的突起, 与唯一的属型种娇晚叉额雷兽(*Epimanteoceras formosus*)明显不同。马氏晚叉额雷兽同属型种关系最近, 两者在系统发育分析中同为雷兽亚族(Brontotheriina)的基干类群, 但是两者是否为后者的姊妹类群尚无法确定。和属型种一样, 马氏晚叉额雷兽在演化程度上与内蒙古伊尔丁曼哈期的谷氏原雷兽(*Protitan grangeri*)接近, 但与同时期地理位置更近的哈萨克斯坦的雷兽*Aktautitan hippopotamopus*相比, 马氏晚叉额雷兽较原始, 表明新种所在的地层时代很可能要早于发现*A. hippopotamopus*地层。三个泉剖面依希白拉组伊尔丁曼哈期内以前发现的化石较少, 此次马氏晚叉额雷兽的发现, 不仅扩大了晚叉额雷兽属的地理分布, 也为依希白拉组内存在伊尔丁曼哈期的沉积提供了新的佐证。

**关键词:** 准噶尔盆地, 三个泉, 中始新世, 晚叉额雷兽

### References

Burger B J, Tackett L, 2014. The stratigraphic importance of the brontothere (cf. *Diplacodon elatus*) in the Brennan Basin Member of the Duchesne River Formation of Utah. *Foss Rec*, 17: 69–74

Colbert E H, 1938. Fossil mammals from Burma in the American Museum of Natural History. *Bull Am Mus Nat Hist*, 74: 255–436

Eberle J J, 2006. Early Eocene Brontotheriidae (Perissodactyla) from the Eureka Sound Group, Ellesmere Island, Canadian High Arctic—implications for brontothere origins and high-latitude dispersal. *J Vert Paleont*, 26: 381–386

Emry R J, Lucas S G, 2002. Brontothere (Mammalia, Perissodactyla) footprints from the Eocene of the Ily Basin, Kazakhstan. *J Vert Paleont*, 22: 51A

Emry R J, Lucas S G, 2003. New ceratomorphs (Mammalia, Perissodactyla) footprints from the Eocene of the Ily Basin, Kazakhstan. *J Vert Paleont*, 23: 44A

Froehlich D J, 2002. Quo vadis eohippus? The systematics and taxonomy of the Early Eocene equids (Perissodactyla). *Zool J Linn Soc*, 134: 141–256

Granger W D, Gregory W K. 1938. A new titanotherere genus from the Upper Eocene of Mongolia and North America. *Bull Am Mus Nat Hist*, 74: 435–436

Granger W D, Gregory W K, 1943. A revision of the Mongolian titanotheres. *Bull Am Mus Nat Hist*, 80: 349–389

Hatcher J B, 1895. On a new species of *Diplacodon*, with a discussion of the relations of that genus to *Telmatotherium*. *Am Nat*, 29: 1084–1090

Holroyd P A, Ciochon R L, 2000. *Bunobrontops savagei*, a new genus and species of Brontotheriidae perissodactyl from the Eocene Pondaung fauna of Myanmar. *J Vert Paleont*, 20: 408–410

Hu C K, 1961. The occurrence of *Parabrontops* in Hami, Xinjiang. *Vert PalAsiat*, 3: 41–42

Huang X S, Zheng J J, 2004. Brontotheres (Perissodactyla, Mammalia) from the Middle Eocene of Lunan, Yunnan. *Vert PalAsiat*, 42: 334–339

Kazunori M, Yukimitsu T, Beard K et al., 2011. Eocene mammals from the Akasaki and Nakakoshiki formations, Western Kyushu, Japan: preliminary work and correlation with Asian land mammal ages. *Vert PalAsiat*, 49: 53–68

Kumar K, Sahni A, 1985. Eocene mammals from the upper Subathu Group, Kashmir Himalaya, India. *J Vert Paleont*, 5: 153–168

Li Y A, Keyum N, Fang X S et al, 2009. Mesozoic and Cenozoic strata and fossils in the northern Junggar Basin of Xinjiang Uygur Autonomous Region. *Xinjiang Geology*, 27: 21–23

Mader B J, 1989. The Brontotheriidae: a systematic revision and preliminary phylogeny of North American genera. In: Prothero D R, Schoch R M eds. *The Evolution of Perissodactyls*. New York: Oxford University Press. 458–484

Mader B J, 1998. Brontotheriidae. In: Janis C M, Scott K M, Jacobs L L eds. *Evolution of Tertiary Mammals of North America: Terrestrial Carnivores, Ungulates, and Ungulate-like Mammals*. Cambridge: Cambridge University Press. 525–536

Marsh O C, 1872. Preliminary description of new Tertiary mammals. *Am J Sci Arts*, 4: 1–35

Marsh O C, 1875. Notice of new Tertiary mammals. IV. *Am J Sci Arts*, 9: 239–250

Miao D S, 1982. Early Tertiary fossil mammals from the Shinao Basin, Panxian County, Guizhou Province. *Acta Palaeontol Sin*, 21: 527–536

Mihlbachler M C, 2007. *Eubrontotherium clarnoensis*, a new genus and species of brontothere (Brontotheriidae, Perissodactyla) from the Hancock Quarry, Clarno Formation, Wheeler County, Oregon. *Paleobios*, 27: 19–39

Mihlbachler M C, 2008. Species taxonomy, phylogeny, and biogeography of the Brontotheriidae (Mammalia: Perissodactyla). *Bull Am Mus Nat Hist*, 311: 1–475

Mihlbachler M C, Lucas S G, Emry R J et al., 2004. A new brontothere (Brontotheriidae, Perissodactyla, Mammalia) from the Eocene of the Ily Basin of Kazakhstan and a phylogeny of Asian “horned” brontotheres. *Am Mus Novit*, 3439: 1–43

Missiaen P, Gunnell G F, Gingerich P D, 2011. New Brontotheriidae (Mammalia, Perissodactyla) from the Early and Middle Eocene of Pakistan with implications for mammalian paleobiogeography. *J Vert Paleont*, 85: 665–677

Osborn H F, 1907. Tertiary mammal horizons of North America. *Bull Am Mus Nat Hist*, 23: 237–253

Osborn H F, 1923. Titanotheres and lophiodonts in Mongolia. *Am Mus Novit*, 91: 1–5

Osborn H F, 1925. Upper Eocene and Lower Oligocene titanotheres of Mongolia. *Am Mus Novit*, 202: 1–12

Osborn H F, 1929. *Embolotherium*, gen. nov., of the Ulan Gochu, Mongolia. *Am Mus Novit*, 353: 1–20

Qi T, Beard K C, 1996. *Nanotitan shanghuangensis*, gen. et sp. nov.: the smallest known brontothere. *J Vert Paleont*, 16: 578–581

Qi T, Beard K C, 1998. *Nanotitanops*, a new name for *Nanotitan* Qi and Beard, 1996 not *Nanotitan* Sharov, 1968. *J Vert Paleont*, 18: 812

Thewissen J G M, Gingerich P D, Russell D E, 1987. Artiodactyla and Perissodactyla (Mammalia) from the Early–Middle Eocene Kuldana Formation of Kohat (Pakistan). *Contrib Mus Paleont Univ Michigan*, 27: 247–274

Thewissen J G M, Williams E M, Hussain S T, 2001. Eocene mammal faunas from northern Indo–Pakistan. *J Vert Paleont*, 21: 347–366

Tong Y S, 1989a. Some Eocene mammals from the Üqbulak Area of the Junggar Basin, Xinjiang. *Vert PalAsiat*, 27: 182–196

Tong Y S, 1989b. A review of Middle and Late Eocene mammalian faunas from China. *Acta Palaeontol Sin*, 28: 663–682

Tong Y S, Qi T, Ye J et al., 1990. Tertiary stratigraphy of the north of Junggar Basin, Xinjiang. *Vert PalAsiat*, 28: 59–70

Wang B Y, 1978. Perissodactyla from the Late Eocene of Lantian, Shensi. *Prof Pap Stratigr Palaeontol*, 7: 118–121

Wang B Y, 1982. Osteology and phylogenetic relationships of *Rhinotitan mongoliensis*. *Mem Inst Vert Paleont Paleoanthrop Acad Sin*, 16: 1–75

Wang B Y, 2000. A skull of *Embolotherium* (Perissodactyla, Mammalia) from Erden Obo, Nei Mongol, China. *Vert PalAsiat*, 38: 237–240

Wang Y, Wang J W, 1997. A new brontothere from late Middle Eocene of Qufu, Shandong. *Vert PalAsiat*, 35: 68–77

Wang Y Q, Meng J, Beard C K et al., 2010. Early Paleogene stratigraphic sequences, mammalian evolution and its response to environmental changes in Erlan Basin, Nei Mongol, China. *Sci China Earth Sci*, 40: 1277–1286

Wei J M, Tong Y S, 1992. The division of Paleocene and Eocene deposits in the northern Junggar Basin. *Acta Petrol Sinica*, 13: 117–120

West R M, 1980. Middle Eocene large mammal assemblage with Tethyan affinities, Ganda Kas Region, Pakistan. *J Vert Paleont*, 54: 508–533

Xu Y X, Chiu C S, 1962. Early Tertiary mammalian fossils from Lunan, Yunnan. *Vert PalAsiat*, 6: 313–332

Yanovskaya N M, 1953. First discovery of a brontothere in Russia. *Doklady Akademii Nauk. SSSR*, 93: 147–149

Yanovskaya N M, 1957. First discovery of *Rhinotitan*, family Brontotheriidae in the USSR. *Vert PalAsiat*, 1: 187–192

Yanovskaya N M, 1976. *Epimanteoceras amplius* sp. nov. (Mammalia, Perissodactyla, Brontotheriidae) from Mongolia. *Tr Sovmest Sov-Mong Paleontol Eksped*, 5: 38–46

Ye J, 1983. Mammalian fauna from the Late Eocene of Ulan Shireh area, Inner Mongolia. *Vert PalAsiat*, 21: 109–118

#### Appendix 1 Character codes of *Epimanteoceras mae* according to Mihlbachler (2008)

<i>Epimanteoceras mae</i> (IVPP V 20713)							
1?????????	??10? ????2	0120100111	0100000000	1011??????	??1111121	1132143022	?????????? ?????